Downregulated microRNA-222 is correlated with increased p27^{Kip1} expression in a double transgenic mouse model of Alzheimer's disease

XIAOYING WANG[1,2], YANFENG XU[1], HUA ZHU[1], CHUNMEI MA[1], XIAOWEI DAI[1] and CHUAN QIN[1]

[1]Institute of Laboratory Animal Science, Chinese Academy of Medical Sciences and Peking Union Medical College, Beijing 100021; [2]Department of Pathology, The Second Hospital of Shandong University, Jinan, Shandong 250100, P.R. China

Received October 22, 2014; Accepted August 25, 2015

DOI: 10.3892/mmr.2015.4339

Abstract. MicroRNAs (miRNAs) are a group of endogenous non-coding small RNAs that regulate protein expression by binding to the 3' untranslated region (UTR) of target genes. miRNAs are abundantly expressed in the central nervous system and participate in neuronal differentiation and synaptic plasticity. However, the possible roles and associated target genes of miRNAs in Alzheimer's disease (AD) are largely unknown. In the current study, miR-222 was observed to be downregulated in APPswe/PSΔE9 mice (a model for AD) compared with age-matched controls. Furthermore, the downregulation of miR-222 was correlated with increased p27^{Kip1} protein levels. Bioinformatic analysis showed that there was one highly-conserved putative binding site for miR-222 in the 3'-UTR of p27^{Kip1}. Luciferase reporter assays confirmed that p27^{Kip1} was a direct target of miR-222. Consistently, there was an inverse correlation between p27^{Kip1} and miR-222 expression levels in SH-SY5Y cells. In conclusion, these results suggest that the abnormal expression of miR-222 may contribute to dysregulation of the cell-cycle in AD, at least in part by affecting the expression of p27^{Kip1}.

Introduction

Alzheimer's disease (AD) is a fatal incurable neurodegenerative disease that is prevalent worldwide (1). The progressive disease is characterized by the accumulation of plaques formed of short β-amyloid (Aβ) peptides, neurofibrillary tangles inside neurons, loss of neurons in the hippocampus and cerebral cortex, and widespread brain atrophy. AD is the most common form of dementia in the elderly, accounting for 50-70% of the late-onset dementia, with 17-20 million affected worldwide (2). Although several key proteins, such as amyloid precursor protein (APP), β-secretase 1, Tau and presenillin-1 (PSEN1), have been identified to be implicated in AD pathogenesis, the etiology and pathogenesis of AD are not well understood.

MicroRNAs are a group of small (~22 nucleotides) endogenous noncoding RNAs, that function as suppressors of gene expression. By binding to the 3'-UTR of their target genes, miRNAs can induce mRNA degradation or translational repression (3,4). miRNAs are abundant in the brain and crucially important in neurodevelopment and synaptic plasticity (5,6). Increasing evidence has revealed that alterations in miRNA expression may contribute to the initiation and progression of AD (7-11). However, the mechanism underlying the role of microRNAs in AD has not been fully elucidated.

p27^{Kip1} is encoded by cyclin-dependent kinase inhibitor 1B and functions to negatively control cell cycle progression (12,13). Expression of p27^{Kip1} can normally inhibit the phosphorylation of pRb and therefore arrest cell proliferation at G1. A number of studies have shown that disordered expression of cell-cycle markers, including p27^{Kip1}, contributes to the pathogenesis of AD (14,15). However, p27^{Kip1} gene expression regulation is not completely understood. The present study hypothesized that the expression of p27^{Kip1} may be regulated by certain miRNAs, and aimed to elucidate the interactions between miR-222 and p27^{Kip1} in AD

Materials and methods

Animal model. The APPswe/PSΔE9 mice model was purchased from the Jackson Laboratory (Ben Harbor, ME, USA). Briefly, the transgenic mice were established by co-injection of the APPswe and PS1ΔE9 vectors (16). The expression of the transgenes is under the control of the mouse prion protein promoter, which can drive high protein expression in the neurons and astrocytes of the central nervous system (17,18). The APPswe transgene encodes a mouse-human hybrid transgene containing the mouse sequence in the extracellular and intracellular regions, and a human sequence within the Aβ domain with Swedish mutations K594N/M595L. The PS1ΔE9 transgene encodes the exon-9-deleted human PSEN1.

Correspondence to: Professor Chuan Qin, Institute of Laboratory Animal Science, Chinese Academy of Medical Sciences and Peking Union Medical College, 5 Panjiayuan, Nanli, Chaoyang, Beijing 100021, P.R. China
E-mail: qinchuan@pumc.edu.cn

Key words: microRNA, microRNA-222, Alzheimer's disease, p27^{Kip1}, APPswe/PSΔE9 mice

Polymerase chain reaction (PCR) amplification of tail DNA was performed to genotype the mice for the presence of the transgene. The PCR reaction mixture of 20 μl contained 100 ng genomic DNA, 2 μl 10X buffer, 0.4 μl dNTPs (10 mM), 0.5 μl forward and reverse primers (20 μM), and 0.2 U *Taq* DNA polymerase (Sangon Biotech, Shanghai, China). The PCR was performed with pre-denaturation at 95˚C for 3 min, followed by 35 cycles of denaturation at 95˚C for 30 s, annealing at 54˚C for 30 s (for APP) or 52˚C for 40 s (for PS1), elongation at 72˚C for 30 s (for APP) or 60 s (for PS1), and a final extension at 72˚C for 10 min. Primer sequences were as follows: Forward: 5'-GACTGACCACTCGACCAGGTTCTG-3' and reverse: 5'-CTTGTAAGTTGGATTCTCATATCCG-3' for APP (product length, 344 bp); and forward: 5'-AATAGAGAACGG CAGGAGCA-3' and reverse: 5'-GCCATGAGGGCACTAAT CAT-3' for presenilin 1 (product length, 608 bp). The transgenic mice and age-matched controls were housed under controlled illumination (12 h light/dark cycle) in a specific pathogen-free environment (room temperature, 20-22˚C; humidity, 55-60%). Food and water were available *ad libitum*. Eight six month-old transgenic mice and eight age-matched controls were used in this study. The mice were sacrificed by inhalation of 5% isoflurane (RWD Life Science, Shenzhen, China) prior to cervical dislocation. Using small scissors, the head was severed and the skin separated in order to fracture the skull. Using small tweezers, small sections of skull were carefully removed in order to expose the brain. The brain tissue samples were immediately frozen in liquid nitrogen, and stored at -80˚C until protein and RNA extraction was performed. All animal protocols were conducted in accordance with the Guide for the Care and Use of Laboratory Animals of the National Institutes of Health (19). Formal approval of this study was obtained from the Committee on the Ethics of Animal Experiments at The Second Hospital of Shandong University (Jinan, China).

Reverse transcription-quantitative polymerase chain reaction (RT-qPCR). Total RNA from brains and cultured cells was isolated using the mirVanaTM miRNA Isolation kit (AM1560, Ambion, Austin, TX, USA) in accordance with the manufacturer's instructions. The RNA was treated with DNase I (AM1906, Ambion) to eliminate genomic DNA contamination. RNA (1 μg) was reverse transcribed into miRNA cDNA and total cDNA using the miScript Reverse Transcription kit (218061, Qiagen, Hilden, Germany), followed by qPCR on a Lightcycler (Roche Diagnostics, Mannheim, Germany) machine using the miScript SYBR Green PCR kit (218073, Qiagen), according to the manufacturer's instructions. Primers for mature miR-222 and U6snRNA were purchased from Qiagen (MS00007609 and MS00007497, Hilden, Germany). The primer sequence were as follows: Forward: 5'-CAGGT CTCCAAGACGACATAGA-3' and reverse: 5'-CGCCTTT TCGATTCATGTACTGC-3' for p27^{Kip1} (20); and forward: 5'-CATGGGTGTGAACCATGAGA-3' and reverse: 5'-TGT GGTCATGAGTCCTTCCA-3' for GAPDH. All reactions were run in triplicate. Relative expression levels for p27^{Kip1} mRNA and miR-222 were determined using the $2^{-\Delta\Delta Cq}$ method.

Cell culture. The SH-SY5Y and HEK-293T cell lines were obtained from the Cell Bank of Chinese Academy of Sciences (Shanghai, China) and routinely cultured in Dulbecco's modified Eagle's medium (11965-092, Invitrogen Life Technologies, Carlsbad, CA, USA) supplemented with 10% heat-inactivated fetal bovine serum (Invitrogen Life Technologies), 100 U/ml penicillin and 100 μg/ml streptomycin (Sigma-Aldrich, St. Louis, MO, USA) in a humidified air atmosphere of 5% CO_2 at 37˚C.

miR-222 overexpression in cultured cells. Overexpression of miR-222 was performed using an miR-222 expression vector, which was constructed using BLOCK-iTTM Pol II miR RNAi Expression Vector kit with EmGFP (K4936-00, Invitrogen Life Technologies) according to the manufacturer's instructions. The top oligo sequence for miR-222 is 5'-TGCTGAGCTACATCTGGCTACTGGGTGTTTTGGC CACTGACTGACACCCAGTACAGATGTAGCT-3', and the bottom oligo sequence for miR-222 is 5'-CCTGAGCTACA TCTGTACTGGGTGTCAGTCAGTGGCCAAAACACCC AGTAGCCAGATGTAGCTC-3'. The negative control vector was provided by Invitrogen Life Technologies, which contains an insert that can form a hairpin structure just as a regular pre-miRNA, but is predicted not to target any known vertebrate gene. The expression vector or control vector was transfected into the SH-SY5Y cell line with Lipofectamine 2000 reagent (11668-019, Invitrogen Life Technologies). To generate the stable cell line that can constitutively express miR-222, blasticidin (15205, Sigma-Aldrich) was added 24 h after transfection at concentration of 3 μg/ml for 10 days. Resistant cells were analyzed by fluorescent microscopy (TE2000-U; Nikon Corporation, Tokyo, Japan).

miR-222 knockdown in cultured cells. The inhibition of miR-222 in SH-SY5Y cells was produced with the locked nucleic acid (LNA) oligonucleotides for specific *in vitro* knockdown. The LNA oligonucleotides (exhibiting high affinity to complementary nucleic acids and able to efficiently silence their target miRNAs *in vitro* and *in vivo*) were purchased from Exiqon (Vedbaek, Denmark) and transfected with Lipofectamine 2000 reagent (11668-019, Invitrogen Life Technologies, Carlsbad, CA, USA) at a final concentration of 80 nM. The cells were collected 48 h after transfection, and the levels of miR-222 and p27^{Kip1} were analyzed.

Dual-luciferase reporter assay. The analysis by the miRNA target prediction algorithm TargetScan (http://www.targetscan.org/) revealed that p27^{Kip1} is a candidate target gene of miR-222. The 3'-UTR of human p27^{Kip1} was amplified by PCR using the following primers 5'-TAAGAATATGTTTCCTTGTTTATCAGAT-3' and 5'-AATAGCTATGGAAGTTTTCTTTATTGAT-3'. The PCR products were directionally cloned downstream of the *Renilla* luciferase stop codon in the psiCHECKTM-2 vector (C-8021, Promega Corporation, Madison, WI, USA). The 3'-UTR of the mutant vector of p27^{Kip1} was also constructed by the overlap extension PCR method using the following primers: 5'-CTCT AAAAGCGTTGGAGCATTATGCAATTAGG-3' and 5'-CCTAATTGCATAATGCTCCAACGCTTTTAGAG-3'. The wild-type or mutant p27^{Kip1} 3'-UTR psiCHECK-2 plasmid was transiently co-transfected with miR-222 expression vector or negative control vector into HEK-293T cells. Cell lysates were harvested 48 h after transfection and then firefly and

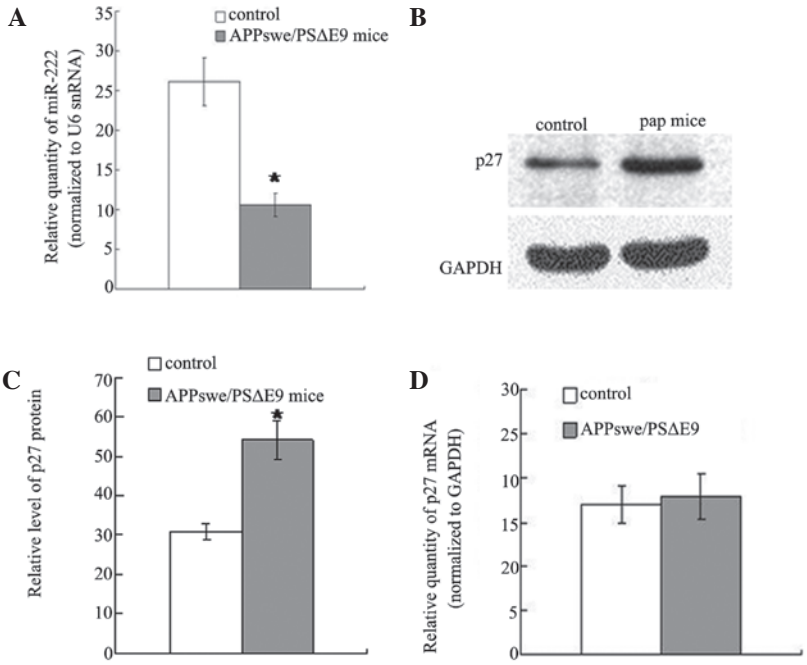

Figure 1. Expression of miR-222 and $p27^{Kip1}$ in the cerebral cortex of APPswe/PSΔE9 mice and controls. (A) The level of miR-222 in the cerebral cortex of APPswe/PSΔE9 mice and controls was determined by RT-qPCR. Data were normalized based on the detection of U6snRNA in the various samples. Statistical analysis was performed using Student's t-test. *P<0.05. (B) GAPDH and $p27^{Kip1}$ proteins were measured from cerebral cortex of APPswe/PSΔE9 (pap) mice and controls using western blot analysis. (C) Semi-quantitative analyses of western blots for $p27^{Kip1}$ protein. The data are presented as the mean ± standard deviation. *P<0.05. (D) $p27^{Kip1}$ mRNA in cerebral cortex of APPswe/PSΔE9 mice and controls was measured by RT-qPCR. The data were normalized based on the detection of GAPDH in the various samples. miR, microRNA; RT-qPCR, reverse transcription-quantitative polymerase chain reaction.

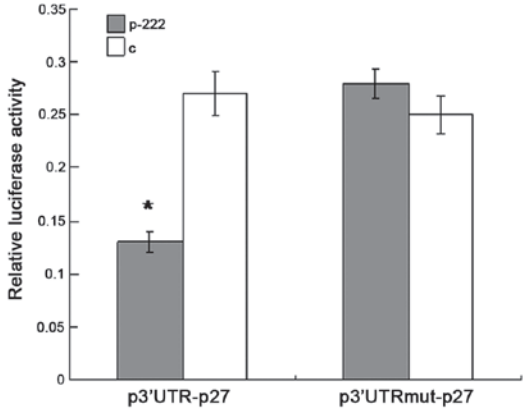

Figure 2. Interaction of miR-222 with the 3'UTR of $p27^{Kip1}$ mRNA. p3'UTR-p27 or p3'UTRmut-p27 luciferase constructs containing a wild-type or a mutated $p27^{Kip1}$ 3'UTR were cotransfected into HEK-293T cells with the miR-222 expression vector (P-222) or negative control vector. Luciferase activity was determined 48 h after transfection. The ratio of normalized sensor to control luciferase activity is shown. Error bars represent the standard deviation and were obtained from three independent experiments. *P<0.05. miR, microRNA; UTR, untranslated region.

Renilla luciferase was measured with the Dual Luciferase Reporter Assay system (E1910, Promega Corporation) following the manufacturer's instructions. *Renilla* luciferase activities were normalized to firefly luciferase activities to also control transfection efficiency.

Western blot analysis. The cells and tissues were homogenized in chilled radioimmunoprecipitation assay lysis buffer (Beyotime Institute of Biotechnology, Shanghai, China) and stood for 30 min on ice. After centrifugation at 17,530 x g for 30 min at 4˚C, the supernatants were collected as protein samples. The protein concentration was detected by the BCATM Protein Assay kit (Pierce, Biotechnology Inc., Rockford, IL, USA). Proteins (40 μg) were separated on 12% SDS-PAGE gels (Thermo Fisher Scientific, Inc., Waltham, MA, USA), and transferred to nitrocellulose membranes (Millipore, Billerica, MA, USA). The membranes were blocked with 5% non-fat milk for 2 h, and incubated overnight at 4˚C with mouse monoclonal anti-human/mouse primary antibody against $p27^{Kip1}$ (1:250; cat. no. ab82264, Abcam, Cambridge, MA, USA) and rabbit polyclonal anti-human/mouse primary antibody against GAPDH (1:500; cat. no. D261392; Sangon Biotech). The membranes were then washed in Tris-buffered saline (TBS) for three times, and incubated for 1 h at room temperature with horseradish peroxidase-conjugated goat anti-mouse/rabbit secondary antibody (1:1,000; cat. no. A0216/A0208; Beyotime Institute of Biotechnology). Subsequent to another three washes in TBS, signals from the bound secondary antibody were generated using the enhanced chemiluminescence solution (Amersham, Piscataway, NJ, USA) and were detected by exposure of the membranes to X-ray films (Kodak, Rochester, NY, USA). The relative signal intensity was quantified by densitometry with UVIPhoto and UVISoft UVIBand Application V97.04 (Uvitech, Cambridge, UK).

Statistical analysis. Statistical analyses were performed with the statistical software package, SPSS, version 17.0 (SPSS, Inc., Chicago, IL, USA). The results are expressed as the mean ± standard deviation of three independent experiments.

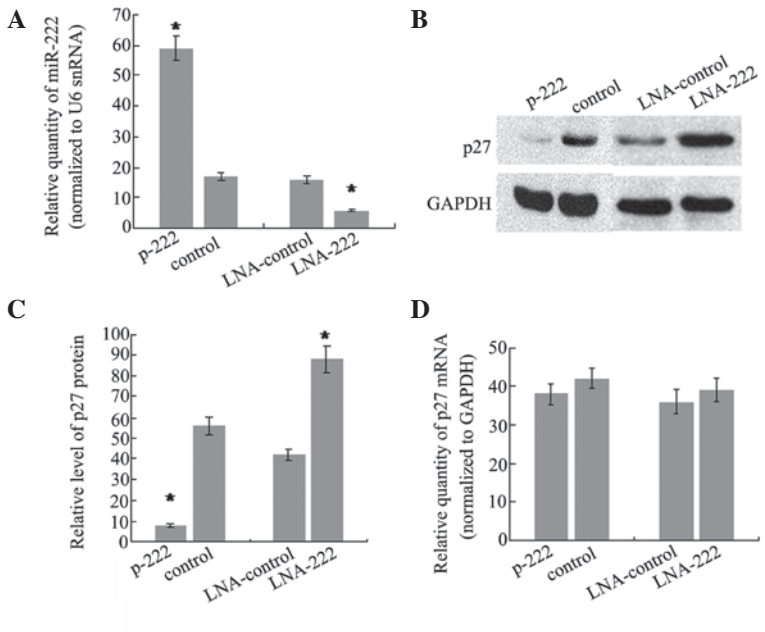

Figure 3. Effects of ectopic miR-222 expression and miR-222 knockdown in SH-SY5Y cells. (A) The level of miR-222 was measured by RT-qPCR. Total RNA was extracted from SH-SY5Y cells transfected with miR-222 expression vector (P-222), negative control vector (control), LNA antisense oligonucleotides targeting miR-222 (LNA-222), or LNA oligos against a microRNA not expressed in these cells (LNA-control) *P<0.05. (B) Representative western blots for p27^{Kip1} in the same SH-SY5Y cells utilized for A. (C) Semi-quantitative analyses of western blots for p27^{Kip1} in the same SH-SY5Y cells utilized for A. Data are presented as the mean ± standard deviation *P<0.05. (D) The level of p27^{Kip1} mRNA was measured by RT-qPCR. Total RNA was extracted from the same SH-SY5Y cells utilized in A. Ct values of p27^{Kip1} were normalized with GAPDH which was served as the reference gene. Error bars represent standard deviation and were obtained from three independent experiments. miR, microRNA; RT-qPCR, reverse transcription-quantitative polymerase chain reaction.

The differences between groups were analyzed by Student's t-test. P-values are two-sided, and P≤0.05 was considered to indicate a statistically significant difference.

Results

miR-222 is downregulated in APPswe/PSΔE9 mice versus control mice. Eight 6-month-old transgenic mice and eight age-matched controls were used in this study. RT-qPCR was performed to evaluate the miR-222 expression level in 8 APPswe/PSΔE9 mice and 8 controls. All reactions were run in triplicate. As shown in Fig. 1A, there was a significantly decreased level of miR-222 in the APPswe/PSΔE9 mice compared with the control group.

Reduced miR-222 is correlated with high level of p27^{Kip1} protein in APPswe/PSΔE9 mice and control mice. To investigate the potential interaction of miR-222 and p27^{Kip1} *in vivo*, western blot analysis was performed on the total protein extracts from the cerebral cortex of 6-month-old APPswe/PSΔE9 mice and controls. It was demonstrated that the level of p27^{Kip1} protein was increased in the APPswe/PSΔE9 mice compared with age-matched controls (Fig. 1B and C), which is inversely associated with the expression of miR-222. In addition, the mRNA level of p27^{Kip1} was also detected by RT-qPCR in the same mice and no significant difference was observed (Fig. 1D). It is well-known that miRNAs execute post-transcriptional regulation by inducing mRNA degradation or translational repression. The present data indicated that low miR-222 expression may positively regulate p27^{Kip1} expression by promoting the translation of p27^{Kip1} mRNA.

3'UTR of p27^{Kip1} mRNA is targeted by miR-222 in HEK-293T cells. To investigate whether p27^{Kip1} is a target gene of miR-222 the alignment of miR-222 with the 3'-UTR of p27^{Kip1} was analyzed by the miRNA target prediction algorithm TargetScan (http://www.targetscan.org/). It was shown that there was one putative binding site in the 3'-UTR of p27^{Kip1}, which has conserved binding sites for miR-222. To experimentally validate the potential interaction, a luciferase reporter containing the 3'-UTR of human p27^{Kip1} was cotransfected into HEK-293T cells with the miR-222-expression vector or negative control vector. The luciferase activity was measured 48 h post transfection. As shown in Fig. 2, the overexpression of miR-222 produced a highly significant reduction (54%, P<0.05) in luciferease activity of the reporter plasmid compared with the controls. In addition, when the predicted binding site of miR-222 in the 3'-UTR was mutated by overlapping PCR, the repression of luciferease activity caused by miR-222 overexpression was abrogated. Collectively, the data suggest that p27^{Kip1} is a predicted target of miR-222, and the inhibitory effect of miR-222 is due to direct interaction with the putative binding site of the 3'-UTR of p27^{Kip1}.

miR-222 regulates p27^{Kip1} expression in SH-SY5Y cells. To further determine whether miR-222 can directly regulate p27^{Kip1}, the changes in the p27^{Kip1} level in SH-SY5Y cells following miR-222 overexpression were analyzed. To do this, the stable transfectant cell line of miR-222, which showed a 3.5-fold increase in miR-222 levels compared with controls (Fig. 3A), was generated. In addition, western blot analysis was performed on the same cells to evaluate the protein level of p27^{Kip1}. The results showed that there was a significant

reduction in the $p27^{Kip1}$ protein level (86%, $P<0.05$) in the stable transfection cell line of miR-222, as compared with cells transfected with the control vector (Fig. 3B and C). Furthermore, miR-222 expression was knocked down by transfecting SH-SY5Y cells with LNA antisense oligonucleotides targeting miR-222 and the effects on $p27^{Kip1}$ production were analyzed. There was a 2.7-fold decrease of miR-222 level in SH-SY5Y cells transfected with anti-222 LNA compared with cells transfected with LNA against a microRNA not expressed in these cells (Fig. 3A). As expected, the reduction of miR-222 was accompanied by an increase in $p27^{Kip1}$ protein of 2.1-fold (Fig. 3B and 3C). It is well-understood that repression of gene expression by miRNAs may be due to translational repression or mRNA degradation. To test the relative contribution of the two mechanisms, the $p27^{Kip1}$ mRNA level was detected and no significant difference was observed following overexpression or knockdown of miR-222. The data demonstrated that miR-222 may regulate $p27^{Kip1}$ expression by interfering with translation of $p27^{Kip1}$ mRNA, rather than inducing mRNA degradation.

Discussion

miRNAs are small non-coding RNA molecules, ~22 nucleotides in length, that regulate gene expression by repressing translation or degrading target mRNAs. miRNAs are abundantly expressed in the brain, where they regulate diverse neuronal and glial functions (4). Numerous types of miRNAs have been recognized to be correlated with neurodegenerative diseases (21-23). miR-222 is a member of the to the miR-221/222 family and has been identified to be overexpressed in several types of cancer (24-27). Growing evidence has indicated the important roles of miR-222 in tumor proliferation, drug resistance, apoptosis and metastasis (28-30). However, for miR-222, the possible roles and associated target genes in AD is unclear. In the current study, it was observed that miR-222 is downregulated in APPswe/PSΔE9 mice compared with age-matched controls. In addition, the overexpression of miR-222 or its knockdown produced the predictable opposite effects on $p27^{Kip1}$ expression. Through the luciferase assay, it was demonstrated that miR-222 can directly target $p27^{Kip1}$ by interaction with the putative binding site of the 3'-UTR of $p27^{Kip1}$.

Previous studies have reported that the dysregulation of cell-cycle markers is important in AD pathogenesis (31-39). $p27^{Kip1}$, also termed cyclin-dependent kinase inhibitor 1B, can prevent cell-cycle progression from the G1 to S phase by binding to CDK2 and cyclin E complexes. Extensive evidence has suggested that the overexpression of $p27^{Kip1}$ is correlated with the pathogenesis of AD. However, $p27^{Kip1}$ gene expression regulation is not completely understood. The present study analyzed the expression of $p27^{Kip1}$ in the cerebral cortex of APPswe/PSΔE9 mice and demonstrated that the protein level of $p27^{Kip1}$ is upregulated in these mice compared with age-matched controls. However, there was no significant difference in mRNA level of $p27^{Kip1}$ between the model mice and controls. This indicates that $p27^{Kip1}$ mRNA may be regulated through a post-transcriptional mechanism. Sequence analysis by Targetscan suggested that the 3'-UTR of $p27^{Kip1}$ mRNA contained a predicted binding site for miR-222. An inverse correlation between the expression of miR-222 and $p27^{Kip1}$ was identified in the model mice and controls. Additionally, there was an inverse correlation between the $p27^{Kip1}$ and miR-222 expression levels in SH-SY5Y cells. Collectively, the results indicated that $p27^{Kip1}$ is a direct target of miR-222 and the downregulation of miR-222 may contribute to the dysregulation of the cell cycle in AD due to dysregulation of the expression of $p27^{Kip1}$.

In conclusion, it was confirmed that miR-222 was downregulated in AD, in association with $p27^{Kip1}$ upregulation. miR-222 can directly target $p27^{Kip1}$ by binding to the 3'-UTR of $p27^{Kip1}$ inducing the translational repression of $p27^{Kip1}$. Therefore, downregulation of miR-222 may be correlated with the dysregulation of the cell cycle in AD by affecting the expression of $p27^{Kip1}$.

Acknowledgements

The authors would like to thank Dr Wei Tong and Dr Xueli Liu for technical assistance, and Dr Jiamei Li, Dr Lingling Zhang, Miss Haixia Shi and Miss Xiaoying Li for their help with research. The present study was supported by grants from the Shandong Provincial Natural Science Foundation of China (grant no. ZR2015PH038).

References

1. Cornutiu G: The Epidemiological Scale of Alzheimer's Disease. J Clin Med Res 7: 657-666, 2015.
2. Blennow K, de Leon MJ and Zetterberg H: Alzheimer's disease. Lancet 368: 387-403, 2006.
3. Kim VN: Small RNAs: Classification, biogenesis and function. Mol Cells 19: 1-15, 2005.
4. Petersen CP, Bordeleau ME, Pelletier J and Sharp PA: Short RNAs repress translation after initiation in mammalian cells. Mol Cell 21: 533-542, 2006.
5. Hébert SS and De Strooper B: Molecular biology. miRNAs in neurodegeneration. Science 317: 1179-1180, 2007.
6. Kosik KS: The neuronal microRNA system. Nat Rev Neurosci 7: 911-920, 2006.
7. Lukiw WJ: Micro-RNA speciation in fetal, adult and Alzheimer's disease hippocampus. Neuroreport 18: 297-300, 2007.
8. Wang WX, Rajeev BW, Stromberg AJ, Ren N, Tang G, Huang Q, Rigoutsos I and Nelson PT: The expression of microRNA miR-107 decreases early in Alzheimer's disease and may accelerate disease progression through regulation of beta-site amyloid precursor protein-cleaving enzyme 1. J Neurosci 28: 1213-1223, 2008.
9. Krichevsky AM, King KS, Donahue CP, Khrapko K and Kosik KS: A microRNA array reveals extensive regulation of microRNAs during brain development. RNA 9: 1274-1281, 2003.
10. Hébert SS and De Strooper B: Alterations of the microRNA network cause neurodegenerative disease. Trends Neurosci 32: 199-206, 2009.
11. Nelson PT, Wang WX and Rajeev BW: MicroRNAs (miRNAs) in neurodegenerative diseases. Brain Pathol 18: 130-138, 2008.
12. Polyak K, Lee MH, Erdjument-Bromage H, Koff A, Roberts JM, Tempst P and Massagué J: Cloning of $p27^{Kip1}$, a cyclin-dependent kinase inhibitor and a potential mediator of extracellular antimitogenic signals. Cell 78: 59-66, 1994.
13. Toyoshima H and Hunter T: p27, a novel inhibitor of G1 cyclin-Cdk protein kinase activity, is related to p21. Cell 78: 67-74, 1994.
14. Ogawa O, Lee HG, Zhu X, Raina A, Harris PL, Castellani RJ, Perry G and Smith MA: Increased p27, an essential component of cell cycle control, in Alzheimer's disease. Aging Cell 2: 105-110, 2003.
15. Delobel P, Lavenir I, Ghetti B, Holzer M and Goedert M: Cell-cycle markers in a transgenic mouse model of human tauopathy: Increased levels of cyclin-dependent kinase inhibitors p21Cip1 and $p27^{Kip1}$. Am J Pathol 168: 878-887, 2006.

16. Jankowsky JL, Fadale DJ, Anderson J, Xu GM, Gonzales V, Jenkins NA, Copeland NG, Lee MK, Younkin LH, Wagner SL, *et al*: Mutant presenilins specifically elevate the levels of the 42 residue beta-amyloid peptide in vivo: Evidence for augmentation of a 42-specific gamma secretase. Hum Mol Genet 13: 159-170, 2004.
17. Borchelt DR, Davis J, Fischer M, Lee MK, Slunt HH, Ratovitsky T, Regard J, Copeland NG, Jenkins NA, Sisodia SS and Price DL: A vector for expressing foreign genes in the brains and hearts of transgenic mice. Genet Anal 13: 159-163, 1996.
18. Lesuisse C, Xu G, Anderson J, Wong M, Jankowsky J, Holtz G, Gonzalez V, Wong PC, Price DL, Tang F, *et al*: Hyper-expression of human apolipoprotein E4 in astroglia and neurons does not enhance amyloid deposition in transgenic mice. Hum Mol Genet 10: 2525-2537, 2001.
19. Mason TJ and Matthews M: Aquatic environment, housing, and management in the eighth edition of the Guide for the Care and Use of Laboratory Animals: Additional considerations and recommendations. J Am Assoc Lab Anim Sci 51: 329-332, 2012.
20. Yang YF, Wang F, Xiao JJ, Song Y, Zhao YY, Cao Y, Bei YH and Yang CQ: MiR-222 overexpression promotes proliferation of human hepatocellular carcinoma HepG2 cells by downregulating p27. Int J Clin Exp Med 7: 893-902, 2014.
21. Kim J, Inoue K, Ishii J, Vanti WB, Voronov SV, Murchison E, Hannon G and Abeliovich A: A MicroRNA feedback circuit in midbrain dopamine neurons. Science 317: 1220-1224, 2007.
22. Schaefer A, O'Carroll D, Tan CL, Hillman D, Sugimori M, Llinas R and Greengard P: Cerebellar neurodegeneration in the absence of microRNA. J Exp Med 204: 1553-1558, 2007.
23. Bilen j, Liu N, Burnett BG, Pittman RN and Bonini NM: MicroRNA pathways modulate polyglutamine-induced neurodegeneration. Mol Cell 24: 157-163, 2006.
24. Galardi S, Mercatelli N, Giorda E, Massalini S, Frajese GV, Ciafrè SA and Farace MG: miR-221 and miR-222 expression affects the proliferation potential of human prostate carcinoma cell lines by targeting $p27^{Kip1}$. J Biol Chem 282: 23716-23724, 2007.
25. Greither T, Grochola LF, Udelnow A, Lautenschläger C, Würl P and Taubert H: Elevated expression of microRNAs 155, 203, 210 and 222 in pancreatic tumors is associated with poorer survival. Int J Cancer 126: 73-80, 2010.
26. Visone R, Russo L, Pallante P, De Martino I, Ferraro A, Leone V, Borbone E, Petrocca F, Alder H, Croce CM and Fusco A: MicroRNAs (miR)-221 and miR-222, both overexpressed in human thyroid papillary carcinomas, regulate $p27^{Kip1}$ protein levels and cell cycle. Endocr Relat Cancer 14: 791-798, 2007.
27. Quintavalle C, Garofalo M, Zanca C, Romano G, Iaboni M, del Basso De Caro M, Martinez-Montero JC, Incoronato M, Nuovo G, Croce CM and Condorelli G: miR-221/222 over-expression in human glioblastoma increases invasiveness by targeting the protein phosphate PTPμ. Oncogene 31: 858-868, 2012.
28. Stinson S, Lackner MR, Adai AT, Yu N, Kim HJ, O'Briene C, Spoerke J, Jhunjhunwala S, Boyd Z, Januario T, *et al*: miR-221/222 targeting of trichorhinophalangeal 1 (TRPS1) promotes epithelial-to-mesenchymal transition in breast cancer. Sci Signal 4: pt5, 2011.
29. Stinson S, Lackner MR, Adai AT, Yu N, Kim HJ, O'Brien C, Spoerke J, Jhunjhunwala S, Boyd Z, Januario T, *et al*: TRPS1 targeting by miR-221/222 promotes the epithelial-to-mesenchymal transition in breast cancer. Sci Signal 4: ra41, 2011.
30. Yang CJ, Shen WG, Liu CJ, Chen YW, Lu HH, Tsai MM and Lin SC: miR-221 and miR-222 expression increased the growth and tumorigenesis of oral carcinoma cells. J Oral Pathol Med 40: 560-566, 2011.
31. Arendt T, Rödel L, Gärtner U and Holzer M: Expression of the cyclin-dependent kinase inhibitor p16 in Alzheimer's disease. Neuroreport 7: 3047-3049, 1996.
32. McShea A, Harris PL, Webster KR, Wahl AF and Smith MA: Abnormal expression of the cell cycle regulators P16 and CDK4 in Alzheimer's disease. Am J Pathol 150: 1933-1939, 1997.
33. Busser J, Geldmacher DS and Herrup K: Ectopic cell cycle proteins predict the sites of neuronal cell death in Alzheimer's disease brain. J Neurosci 18: 2801-2807, 1998.
34. Arendt T, Holzer M and Gärtner U: Neuronal expression of cycline dependent kinase inhibitors of the INK4 family in Alzheimer's disease. J Neural Transm 105: 949-960, 1998.
35. Tsujioka Y, Takahashi M, Tsuboi Y, Yamamoto T and Yamada T: Localization and expression of cdc2 and cdk4 in Alzheimer brain tissue. Dement Geriat Cogn Disord 10: 192-198, 1999.
36. Jordan-Sciutto KL, Malaiyandi LM and Bowser R: Altered distribution of cell cycle transcriptional regulators during Alzheimer disease. J Neuropathol Exp Neurol 61: 358-367, 2002.
37. Hoozemans JJ, Bruckner MK, Rozemuller AJ, Veerhuis R, Eikelenboom P and Arendt T: Cyclin D1 and cyclin E are co-localized with cyclooxygenase 2 (COX-2) in pyramidal neurons in Alzheimer disease temporal cortex. J Neuropathol Exp Neurol 61: 678-688, 2002.
38. Nagy Z, Esiri MM, Cato AM and Smith AD: Cell cycle markers in the hippocampus in Alzheimer's disease. Acta Neuropathol 94: 6-15, 1997.
39. Ding XL, Husseman J, Tomashevski A, Nochlin D, Jin LW and Vincent I: The cell cycle Cdc25A tyrosine phosphatase is activated in degenerating postmitotic neurons in Alzheimer's disease. Am J Pathol 157: 1983-1990, 2000.